Electronic Supplementary Material (ESI) for Dalton Transactions.

Controlling the self-assembly of homochiral coordination architectures of Cu^{II} by the substitution in amino acid based ligands: synthesis, crystal structures and physicochemical properties

Navnita Kumar,[a] Sadhika Khullar,[a,#] and Sanjay K. Mandal*[a]

[a]Department of Chemical Sciences, Indian Institute of Science Education and Research, Mohali, Sector 81, Manauli PO, S.A.S. Nagar, Mohali (Punjab) 140306, INDIA

#Current address: Department of Chemistry, DAV University Jalandhar, (Punjab) 144001, INDIA

Supplementary Information

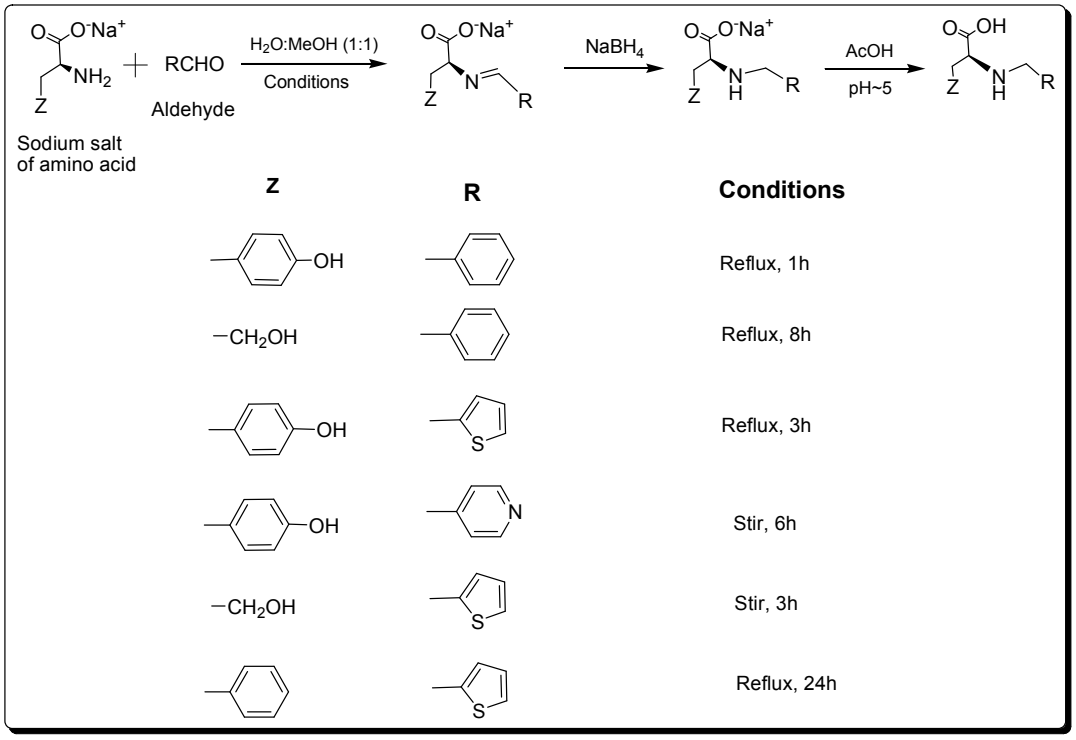

Scheme 1. Synthesis of L-H_2Tyrbenz, L-H_2Serbenz, L-H_2Tyrthio, L-H_2Tyr-4pyr, L-H_2Serthio and L-HPhethio.

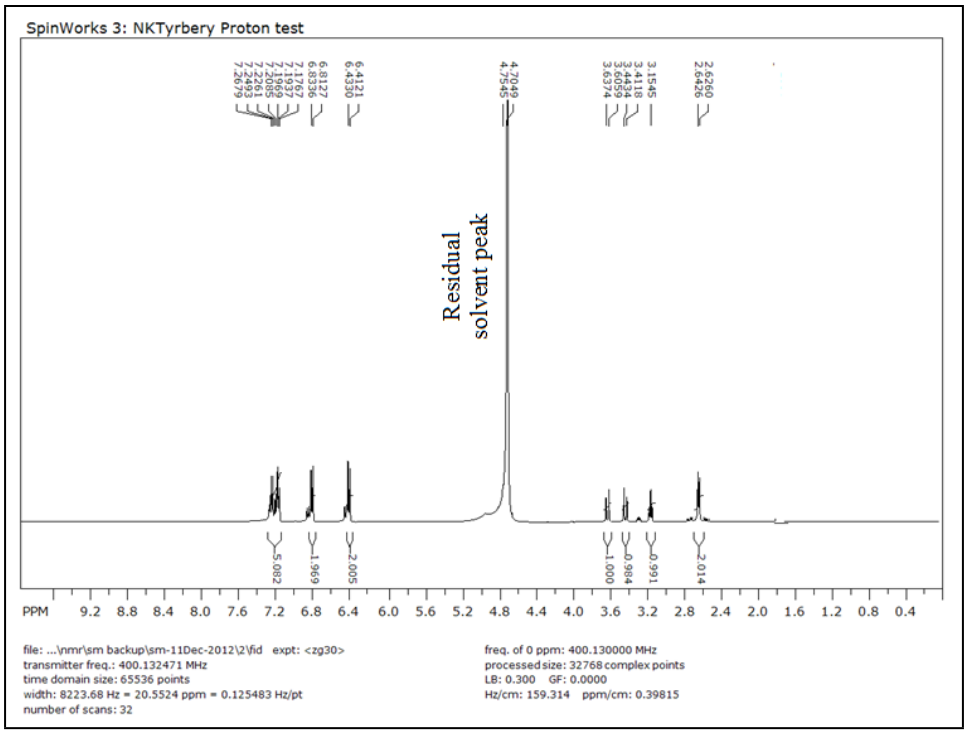

Fig. S1 ^{1}H NMR spectrum of L-NaHTyrbenz.

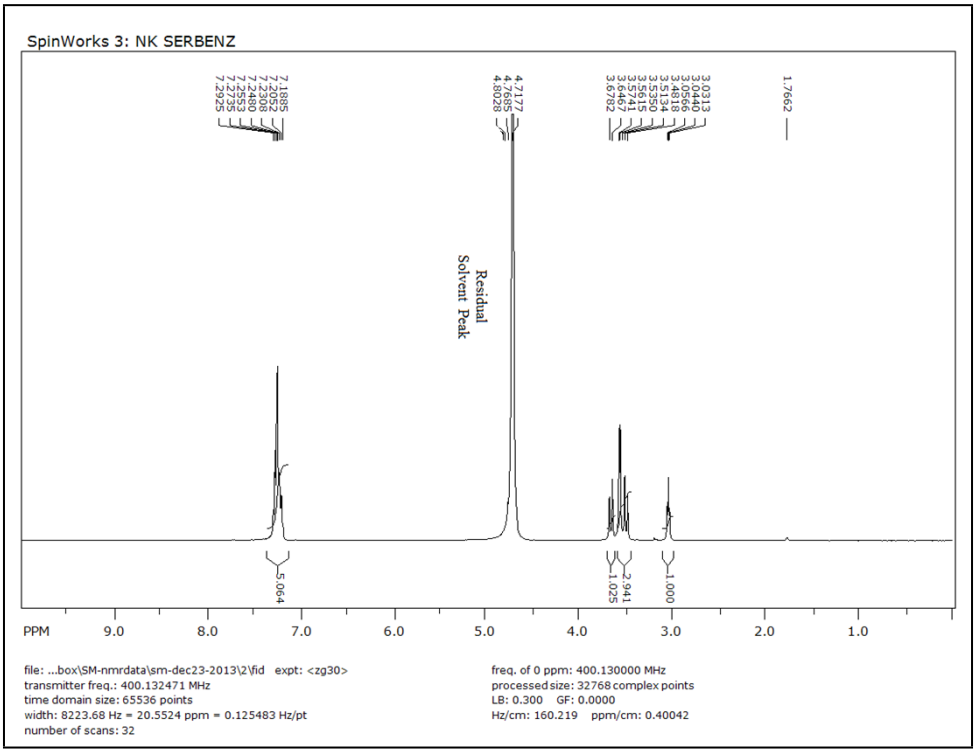

Fig. S2 ^{1}H NMR spectrum of L-NaHSerbenz.

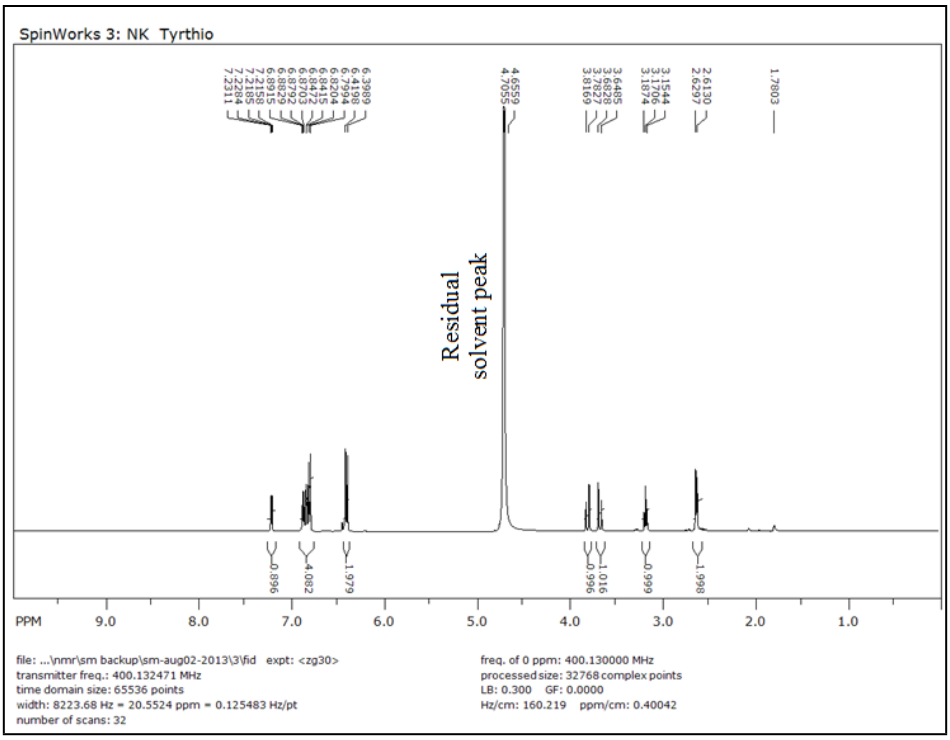

Fig. S3 ^{1}H NMR spectrum of L-NaHTyrthio.

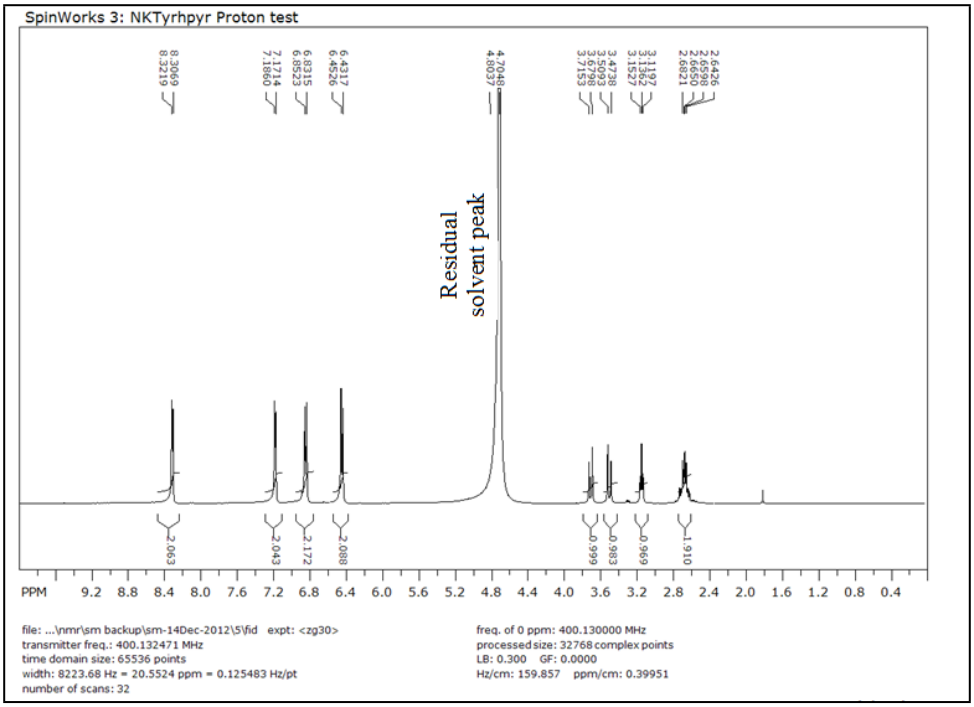

Fig. S4 ^{1}H NMR spectrum of L-NaHTyr4-pyr.

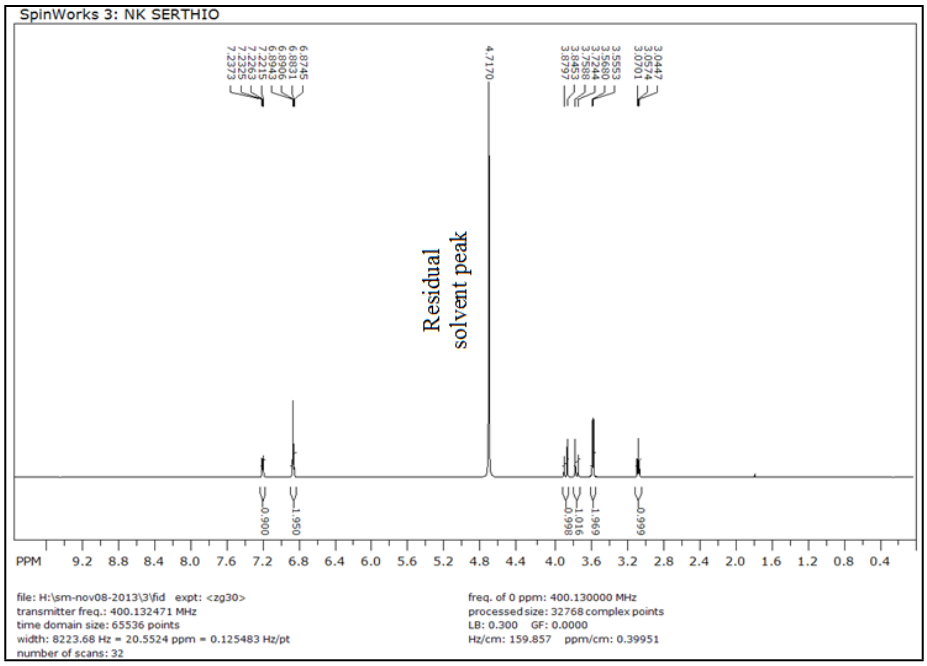

Fig. S5 ^{1}H NMR spectrum of L-NaHSerthio.

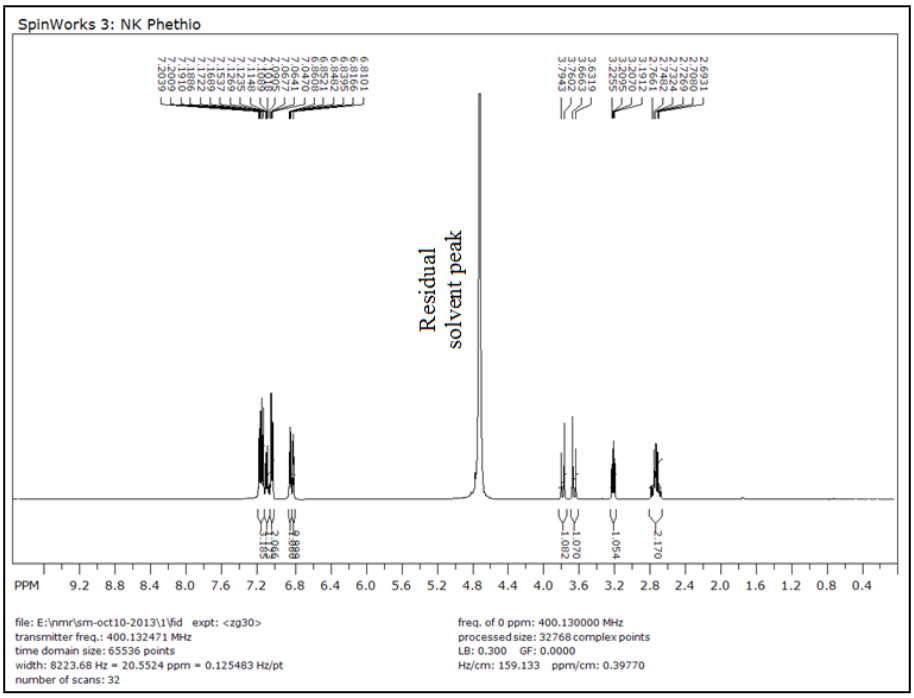

Fig. S6 ^{1}H NMR spectrum of L-NaPhethio.

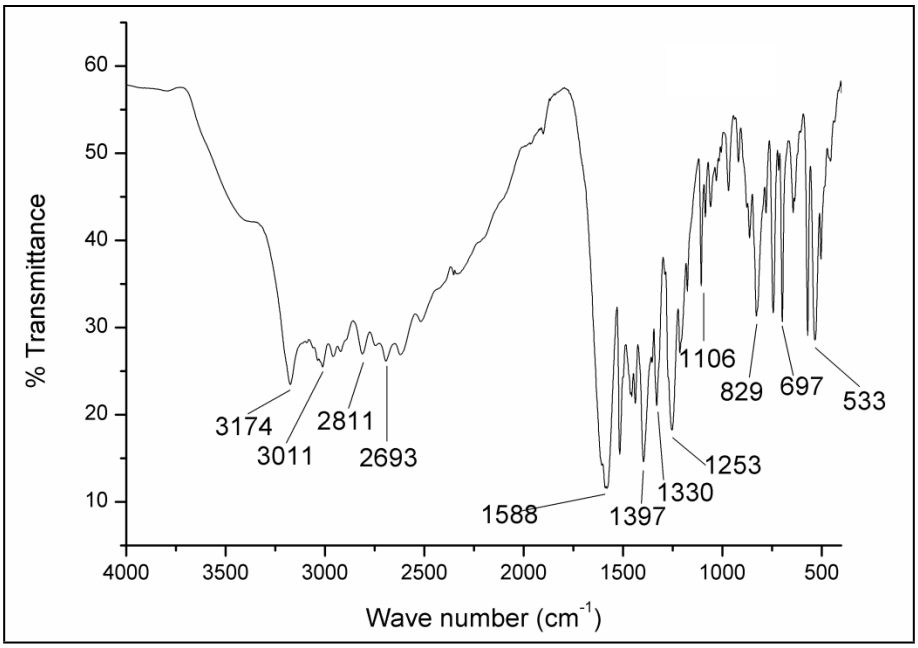

Fig. S7 FTIR spectrum of L-H_2Tyrbenz.

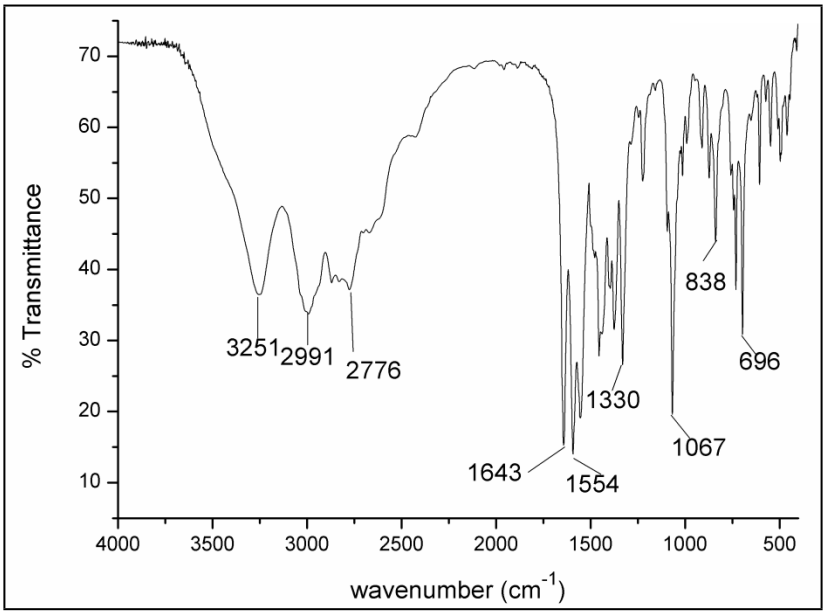

Fig. S8 FTIR spectrum of L-H_2Serbenz.

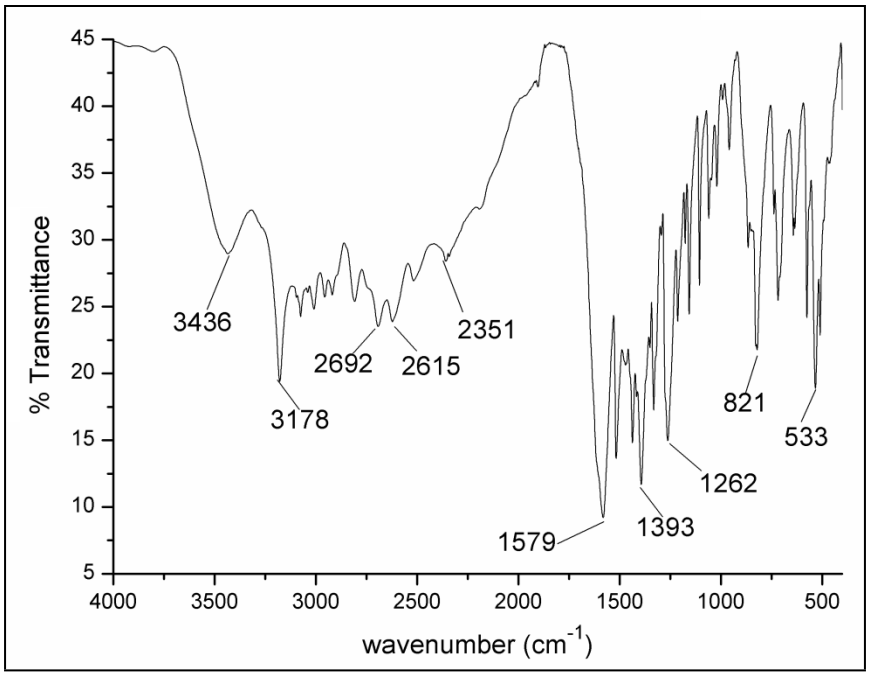

Fig. S9 FTIR spectrum of L-H_2Tyrthio.

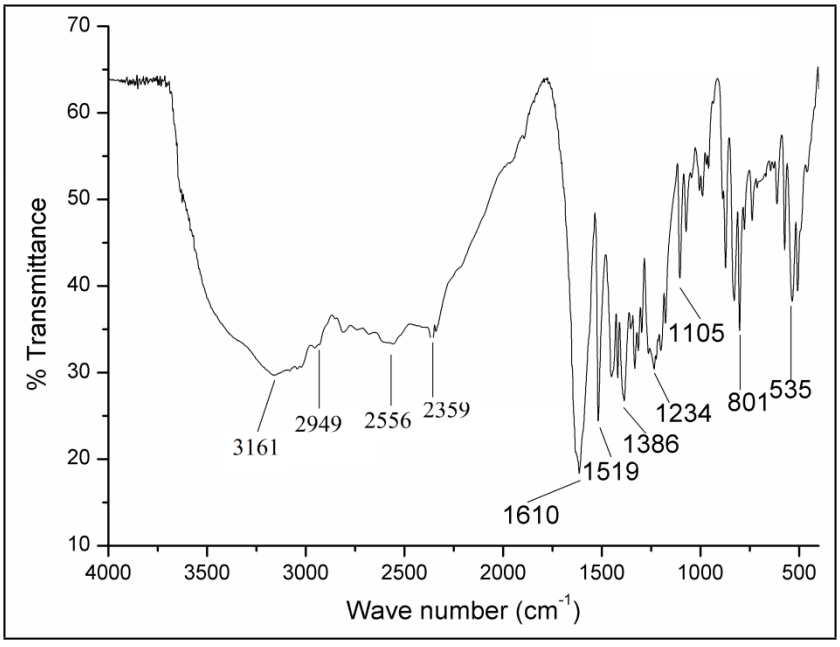

Fig. S10 FTIR spectrum of L-H_2Tyr4-pyr.

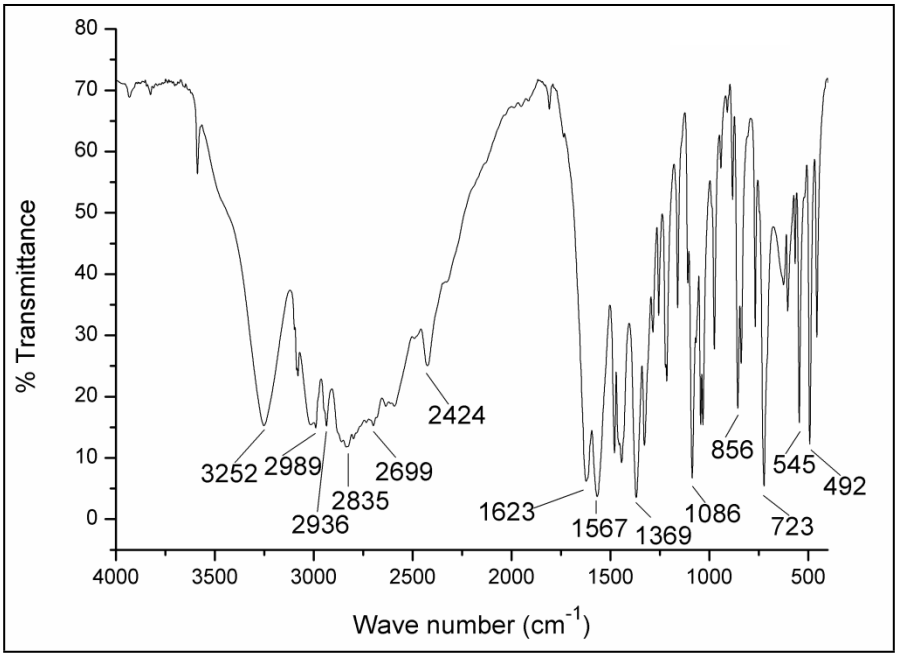

Fig. S11 FTIR spectrum of L-H_2Serthio.

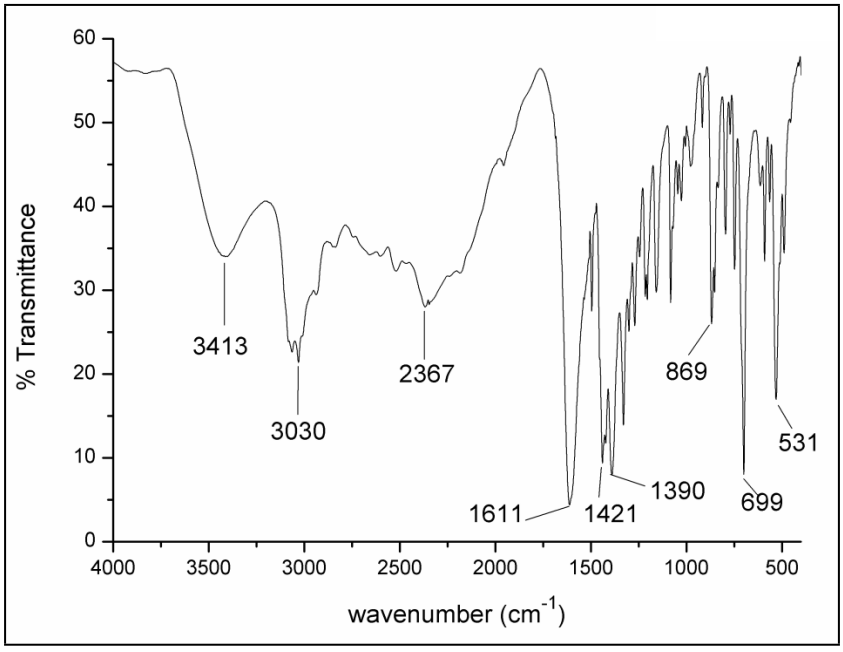

Fig. S12 FTIR spectrum of L-HPhethio.

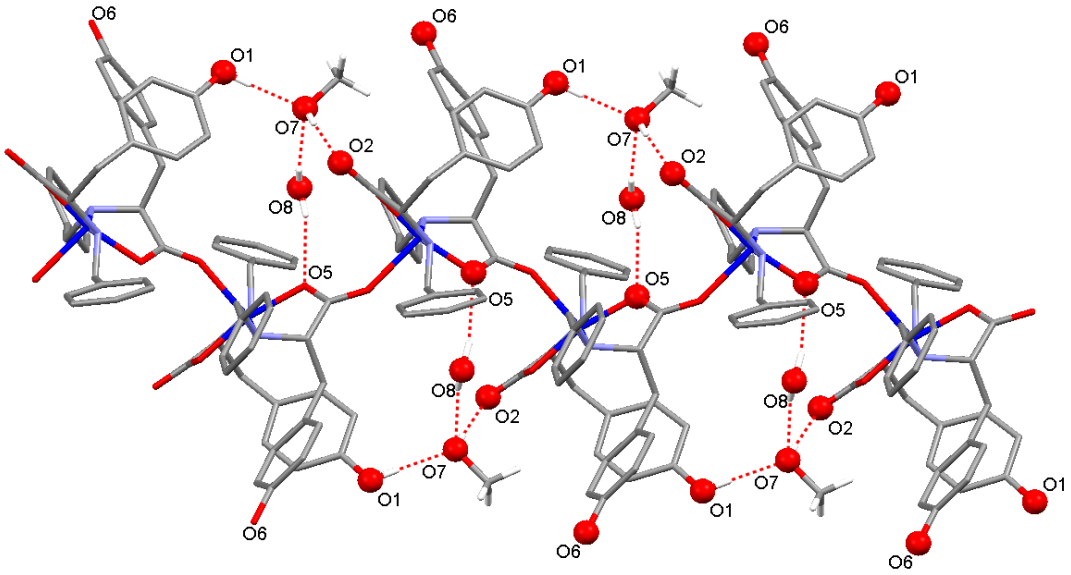

Fig. S13 Hydrogen bonding network within the 1D chain in **1**.

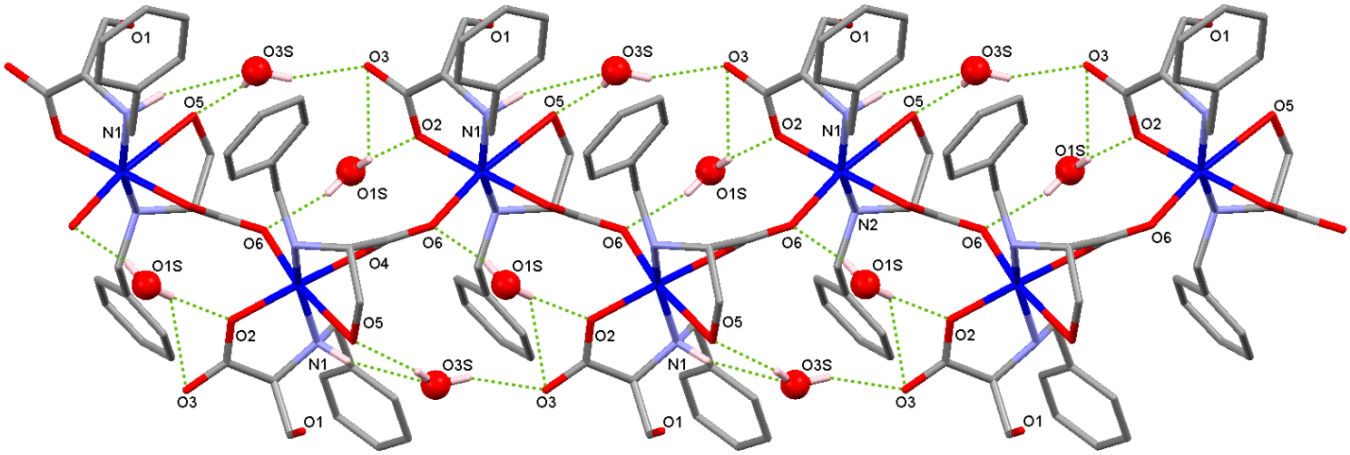

Fig. S14 Hydrogen bonding network within the 1D chain in **2**.

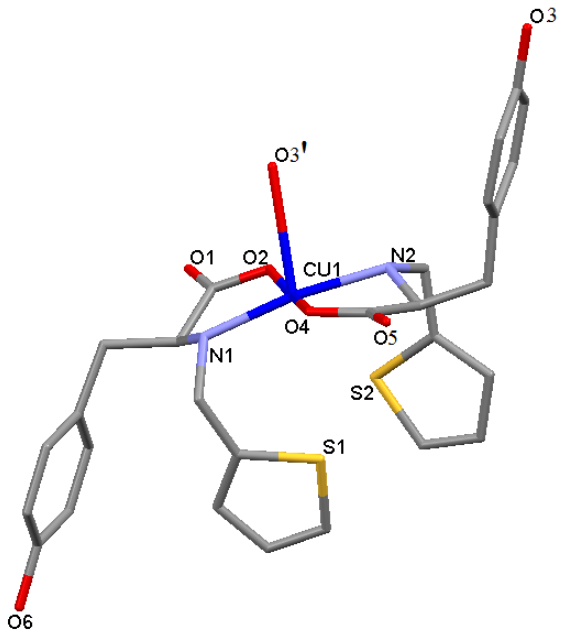

Fig. S15 Coordination environment around Cu(II) in **3**.

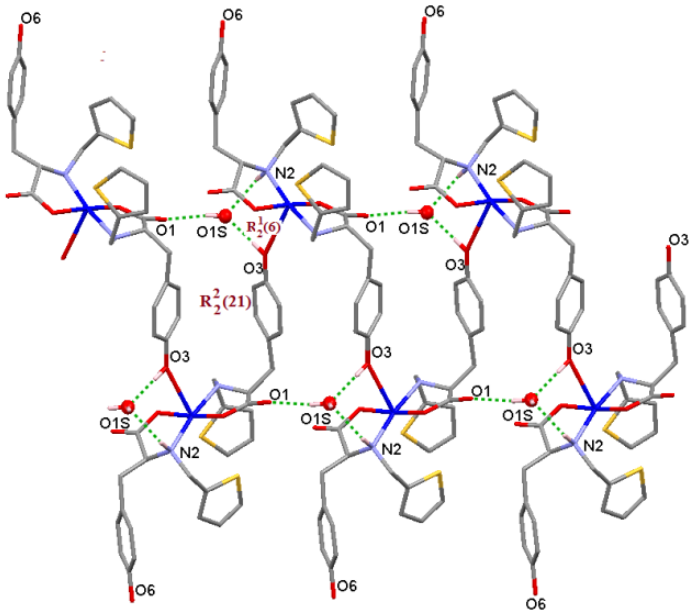

Fig. S16 Hydrogen bonding within the spiral chain in **3**.

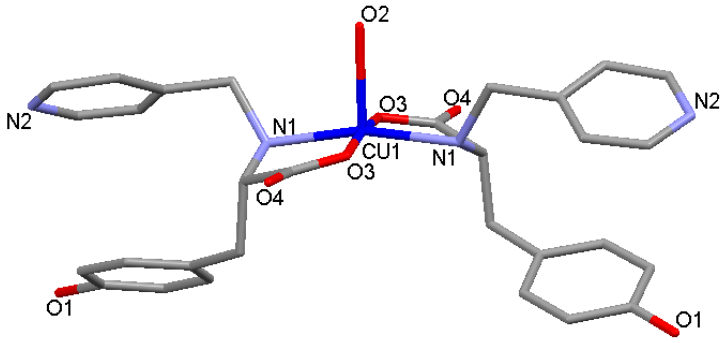

Fig. S17 Coordination environment around Cu(II) in **4**.

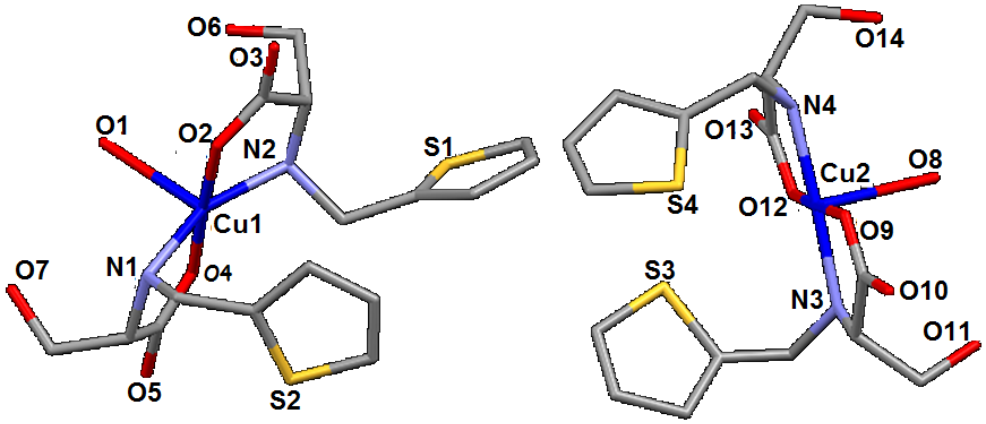

Fig. S18 Coordination environment around Cu(II) in **5** for two independent molecules per asymmetric unit.

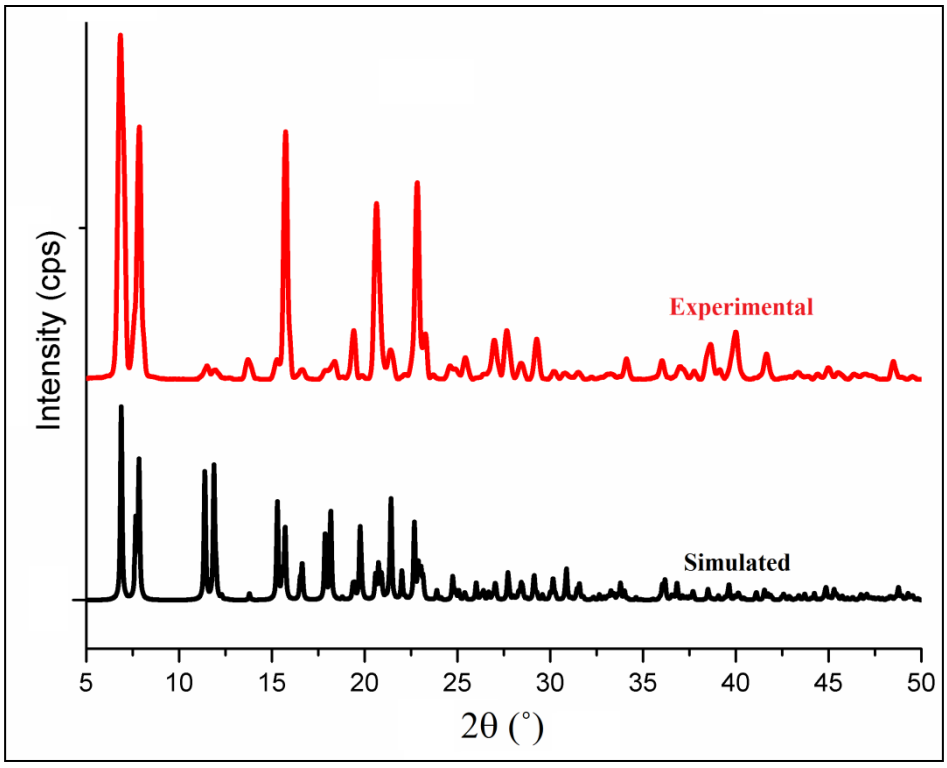

Fig. S19 PXRD patterns of **1**.

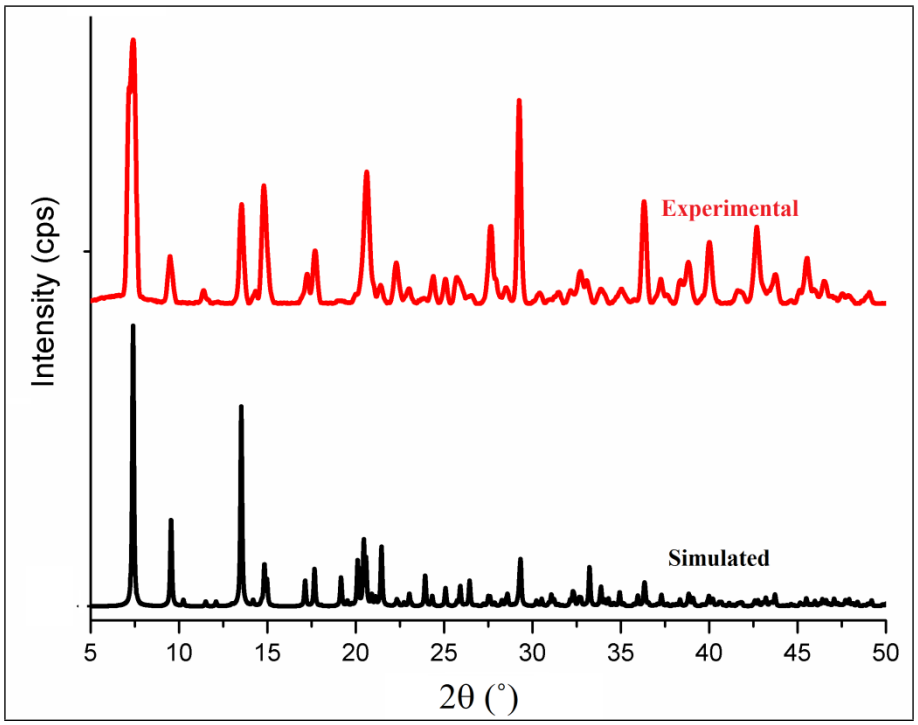

Fig. S20 PXRD patterns of **2**.

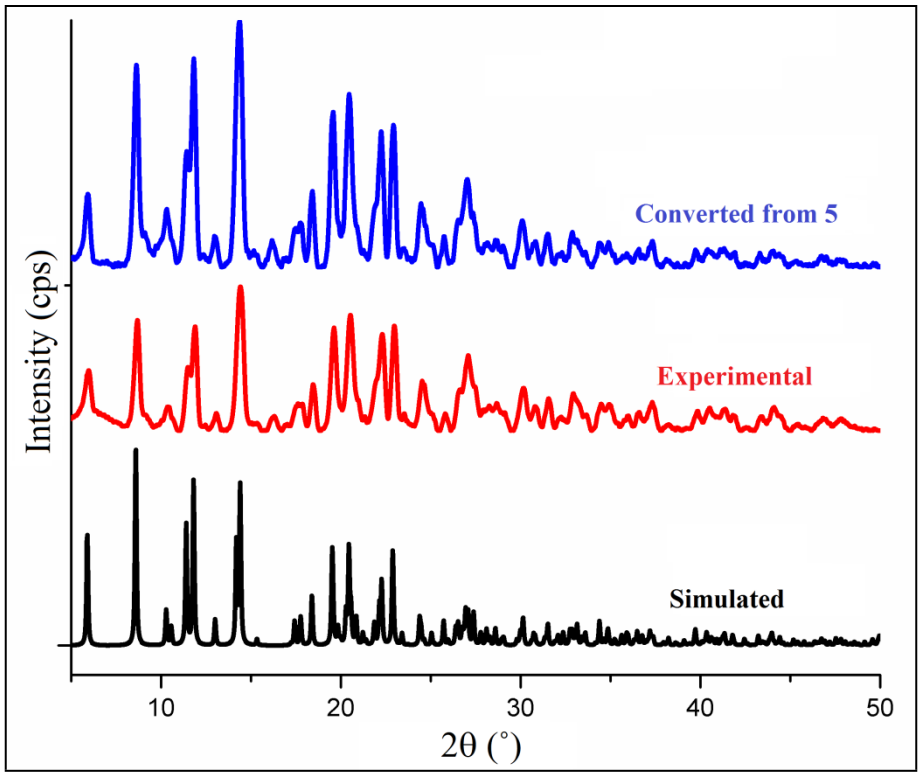

Fig. S21 PXRD patterns of **3**.

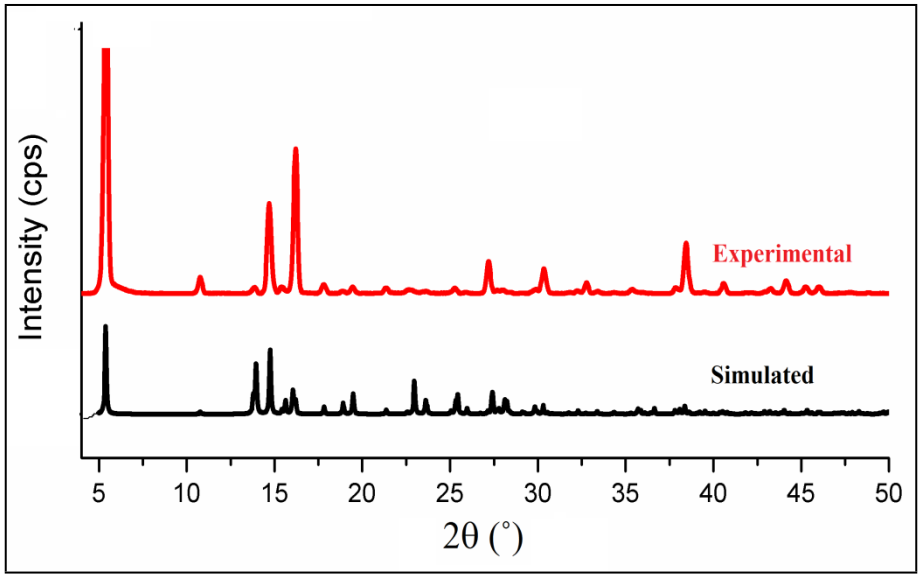

Fig. S22 PXRD patterns of **4**.

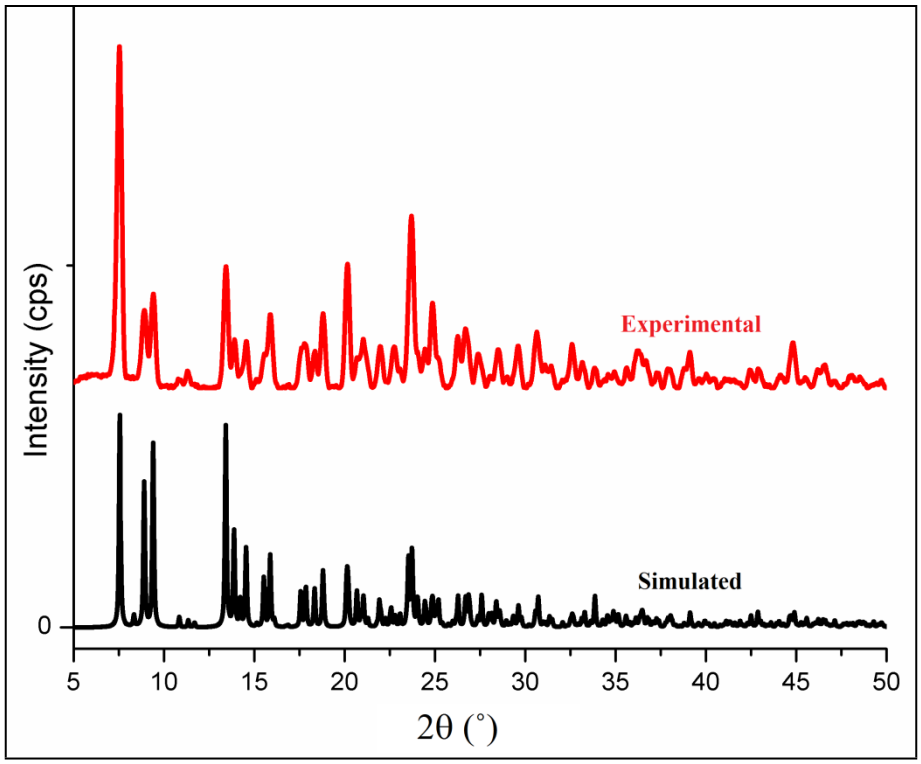

Fig. S23 PXRD patterns of **5**.

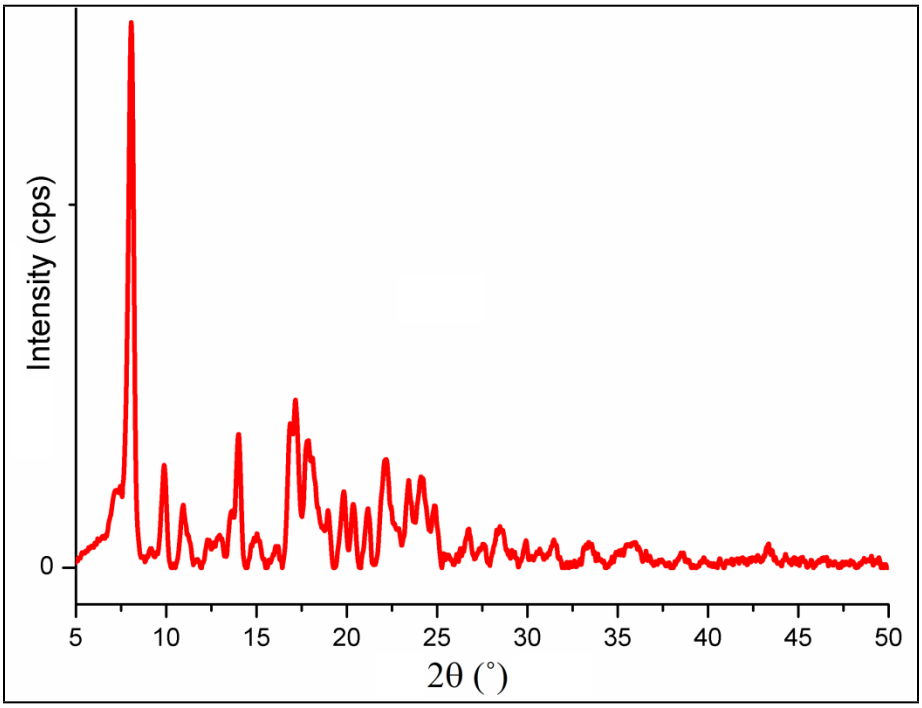

Fig. S24 PXRD pattern of **6**.

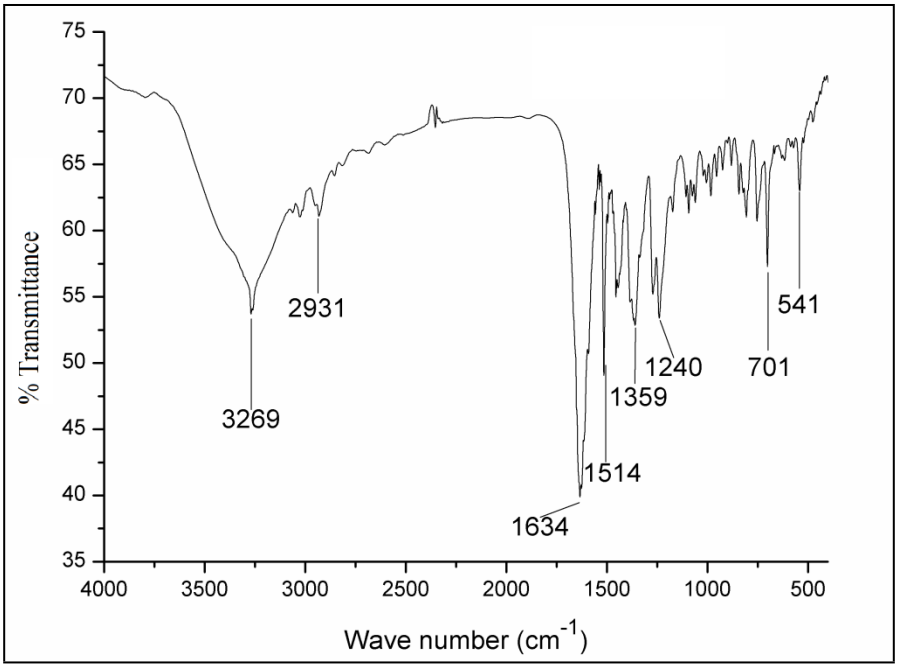

Fig. S25 FTIR spectrum of **1**.

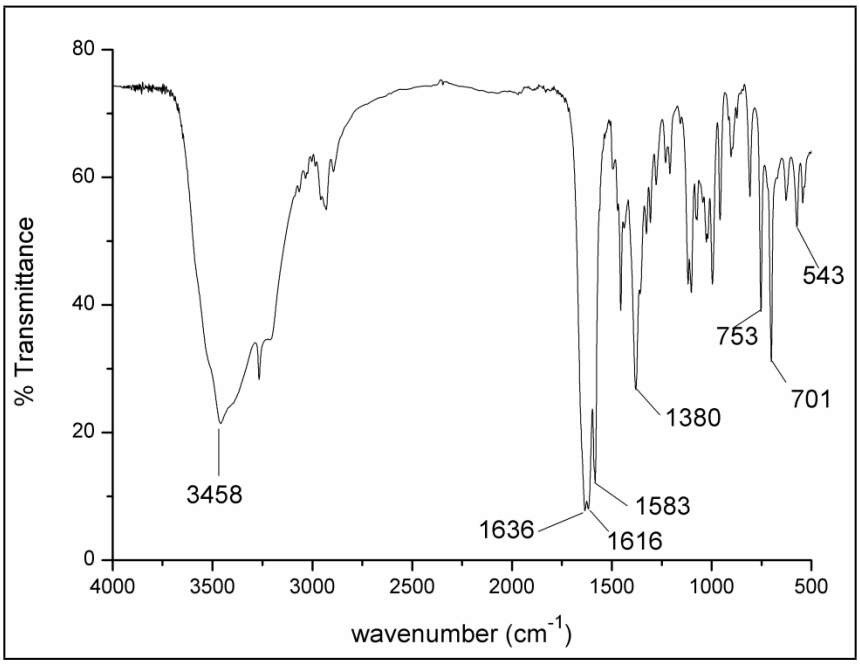

Fig. S26 FTIR spectrum of **2**.

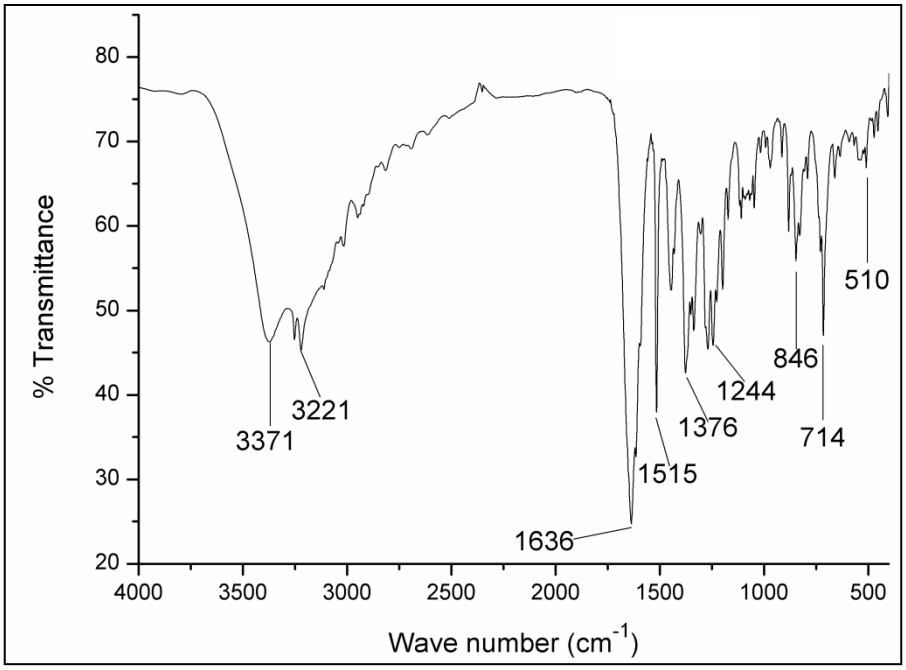

Fig. S27 FTIR spectrum of **3**.

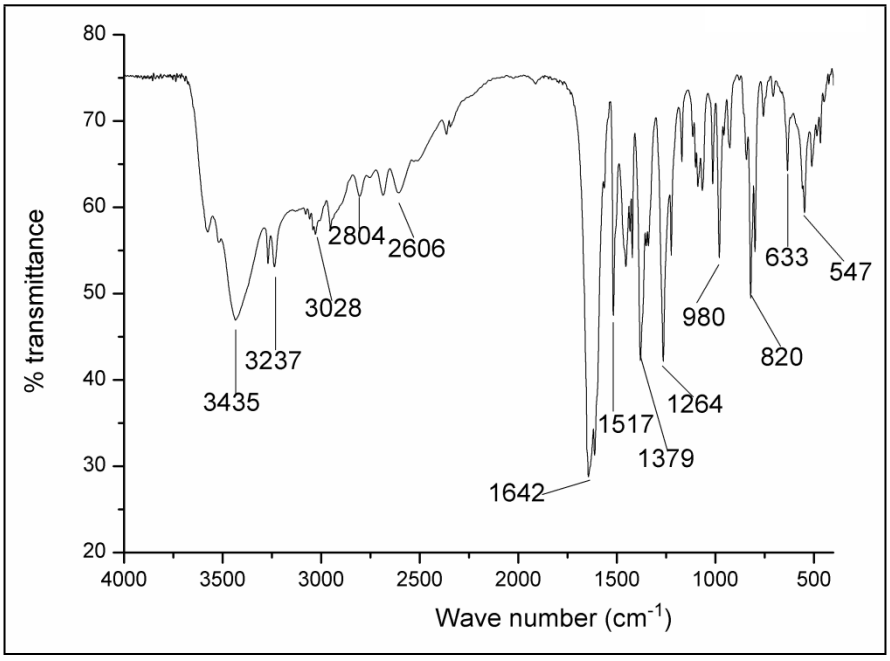

Fig. S28 FTIR spectrum of **4**.

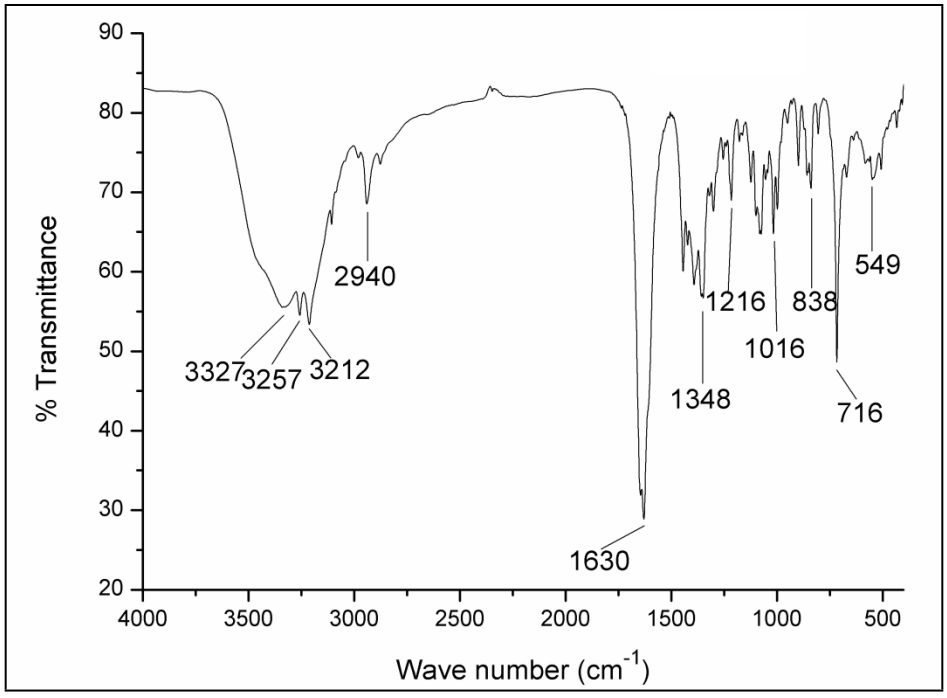

Fig.S29 FTIR spectrum of **5**.

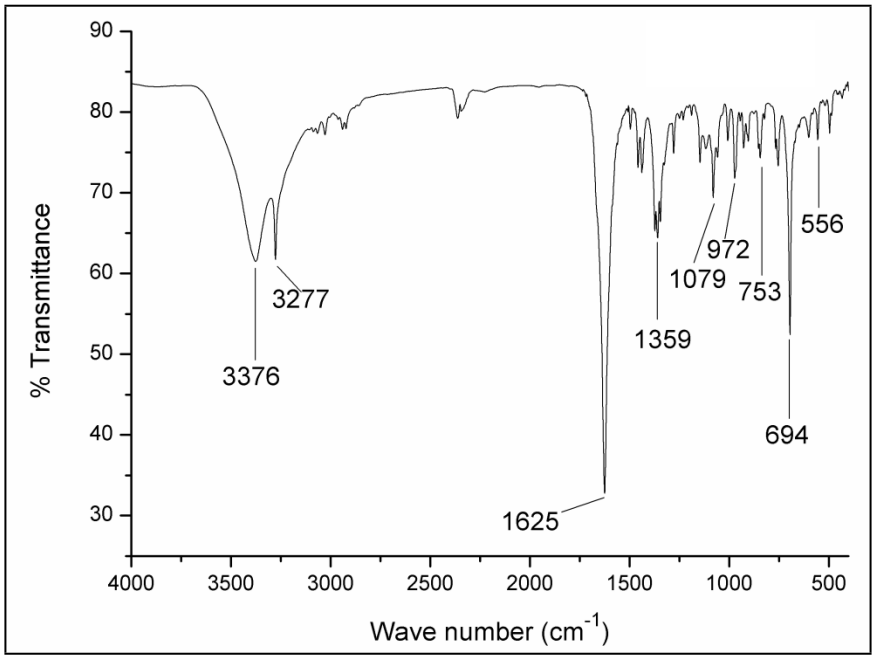

Fig. S30 FTIR spectrum of **6**.

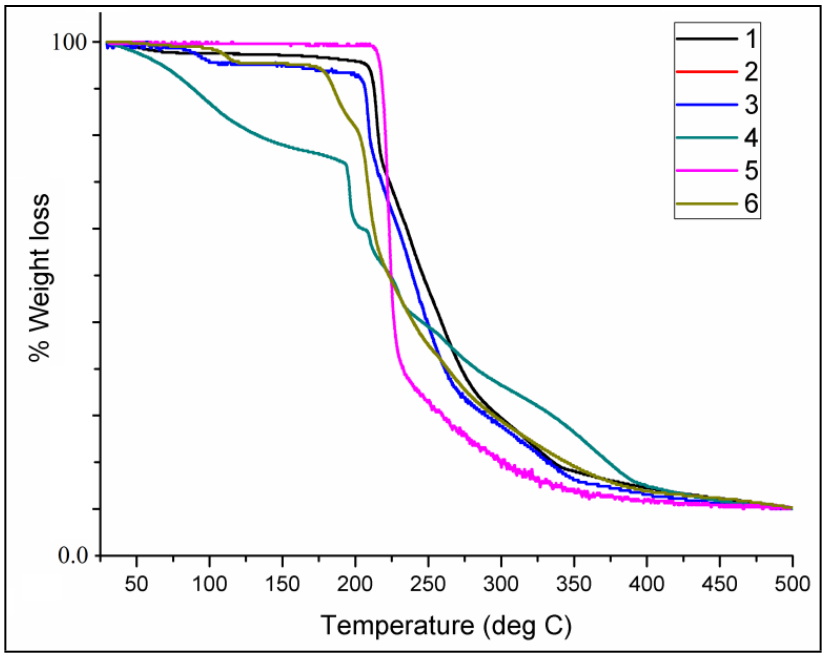

Fig. S31 TGA spectra for **1-6**.

Table S1. Selected Bond lengths (Å) for **1**, **2, 3**, **4** and **5**.

1

Cu1-O3	1.931(3)	Cu1-O5	1.957(3)
Cu1-N2	2.015(3)	Cu1-N1	2.022(3)
Cu1-O4	2.211(4)		

2

Cu1-O2	1.939(3)	Cu1-O4	1.970(3)
Cu1-N1	2.009(4)	Cu1-N2	2.015(3)
Cu1-O6	2.313(3)	Cu1-O5	2.723(1)

3

Cu1-O2	1.901(5)	Cu1-O4	1.929(5)
Cu1-N1	1.997(5)	Cu1-N2	2.030(5)
Cu1-O3’	2.704 (5)		

4

Cu1-O3	1.927(2)	Cu1-O3	1.927(2)
Cu1-N1	2.047(3)	Cu1-N1	2.047(3)
Cu1-O2	2.217(5)		

5

Cu1-O2	1.918(8)	Cu1-O4	1.922(8)
Cu1-N1	1.980(9)	Cu1-N2	2.003(9)
Cu1-O1	2.328(9)	Cu2-O9	1.906(8)
Cu2-O12	1.931(8)	Cu2-N4	1.993(10)
Cu2-N3	1.996(9)	Cu2-O8	2.38(9)

Table S2. Selected Bond angles (degrees) for **1**, **2, 3**, **4** and **5**.

1

O3-Cu1-O5	167.04(15)	O3-Cu1-N2	95.74(14)
O5-Cu1-N2	82.68(14)	O3-Cu1-N1	84.76(16)
O5-Cu1-N1	93.32(15)	N2-Cu1-N1	164.36(17)
O3-Cu1-O4	94.17(15)	O5-Cu1-O4	98.75(14)
N2-Cu1-O4	101.18(14)	N1-Cu1-O4	94.36(15)

2

O2-Cu1-O4	177.84(12)	O2-Cu1-N1	85.00(14)
O4-Cu1-N1	94.02(13)	O2-Cu1-N2	97.71(14)
O4-Cu1-N2	82.48(13)	N1-Cu1-N2	157.76(15)
O2-Cu1-O6	89.97(11)	O4-Cu1-O6	92.03(11)
N1-Cu1-O6	94.78(13)	N2-Cu1-O6	107.25(13)

3

O2-Cu1-O4	171.0(2)	O2-Cu1-N1	84.9(2)
O4-Cu1-N1	93.8(2)	O2-Cu1-N2	99.6(2)
O4-Cu1-N2	82.7(2)	N1-Cu1-N2	172.1(2)

4

O3-Cu1-O3	172.2(3)	O3-Cu1-N1	84.79(11)
O3-Cu1-N1	94.20(11)	O3-Cu1-N1	94.20(11)
O3-Cu1-N1	84.84(11)	N1-Cu1-N1	165.2(2)
O3-Cu1-O2	93.90(13)	O3-Cu1-O2	93.90(13)
N1-Cu1-O2	97.40(11)	N1-Cu1-O2	97.40(11)

5

O2-Cu1-O4	177.7(4)	O2-Cu1-N1	95.9(3)
O4-Cu1-N1	85.3(3)	O2-Cu1-N2	85.1(3)
O4-Cu1-N2	93.1(3)	N1-Cu1-N2	157.7(3)
O2-Cu1-O1	86.6(3)	O4-Cu1-O1	95.4(3)
N1-Cu1-O1	91.6(3)	N2-Cu1-O1	110.7(3)
O9-Cu2-O12	176.2(4)	O9-Cu2-N4	94.1(4)
O12-Cu2-N4	85.1(4)	O9-Cu2-N3	86.1(4)
O12-Cu2-N3	94.9(4)	N4-Cu2-N3	177.7(4)
O9-Cu2-O8	88.3(4)	O12-Cu2-O8	88.0(3)
N4-Cu2-O8	92.1(4)	N3-Cu2-O8	90.2(3)

Table S3. FTIR peaks for carboxylates in **1-6**.

Compound	Carboxylate Peaks (cm^{-1})		$\Delta\upsilon_1$ (cm^{-1})	$\Delta\upsilon_2$ (cm^{-1})	Binding Mode
	Asym	sym			
1	1633 1590	1359 1381	274	 209	monodentate bridging
2	1635 1583	1350 1380	285	 203	monodentate bridging
3	1639	1376	263		monodentate
4	1644	1379	265		monodentate
5	1629	1348	281		monodentate
6	1625	1358	267		monodentate

[$\Delta\upsilon = \upsilon_{asym} - \upsilon_{sym}$]